

Characterization and Simulation of a 915 MHz Receiver

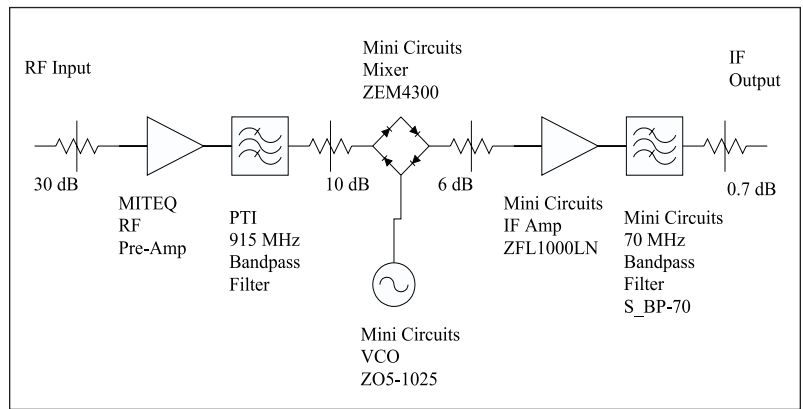
University students learn about wireless design in this thorough study of a receiver subsystem

By Lawrence Dunleavy, Paul Flikkema, Thomas Weller, Anbuselvan Kuppusamy, and E. Benabe
University of South Florida

Students in a new undergraduate course in Wireless Circuits and Systems at the University of South Florida [1] used a versatile test bench and CAE environment to characterize and simulate a 915 MHz receiver subsystem. The subsystem, which down-converts to a 70 MHz IF frequency, is constructed with coaxial components and characterized at several different levels. The 3 GHz test bench includes a vector network analyzer, a spectrum analyzer and a synthesized signal source. Measurements were compared to system simulation using HP EEsof's Advanced Design System (ADS). Simulation accuracy is improved through the use of measured component-level characterization data. This receiver case study provides powerful insight into the capabilities of modern measurement and simulation tools for assessment of system-level linear and nonlinear performance. This revealing case study would be easily duplicated for in-house company training and short course seminars, as well as RF/microwave courses at other universities.

Introduction

Knowledge of the relationships between component and system performance is fundamental to wireless RF/microwave product design. Interestingly, there are few courses that treat both RF/microwave systems and components with a hands-on hardware approach with direct linkage to a modern simulation tool set. A 915



▲ Figure 1. Block diagram of the 915 MHz receiver subsystem.

MHz receiver subsystem was developed in the framework of this new class.

The subsystem, shown in Figure 1, is composed of coaxial components that can readily be characterized individually and assembled to function as a downconverter. The subsystem is studied in detail through a variety of component- and subsystem-level characterization measurements, as well as system simulations using a modern CAE tool set.

The equipment shown in Figure 2 is contained in a new learning environment at USF called the *Wireless and Microwave Instructional Laboratory* ("WAMI" Lab). In the work described here, characterization measurements were made using primarily the HP8714 vector network analyzer (VNA), which features both broadband and narrow-band detection modes and an upper frequency of 3 GHz. Also used was an HP8594E spectrum analyzer (SA) with an upper frequency of 2.9 GHz. During system evaluation and testing, the input is either con-

915 MHz RECEIVER

nected to port 1 of the VNA or to an antenna, for reception of lab-generated signals (via an HP8648C signal source), as well as unwanted “real-world” signals. The output is either connected to the receive port of the VNA for swept-power or swept-frequency measurements, or to the SA for analysis of signal frequency and amplitude content under CW conditions.

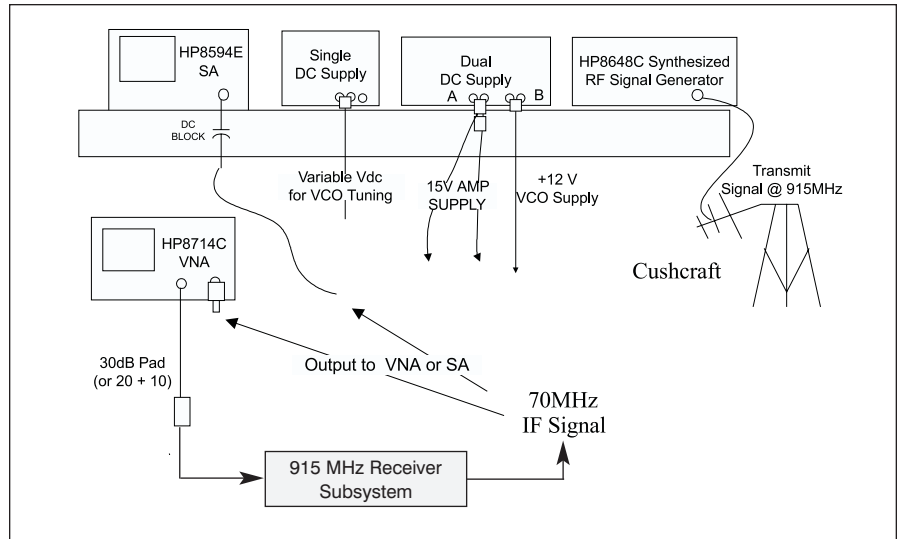
In this design, measurements and simulations were made of two complete receiver assemblies, differing only in component serial numbers, denoted Sys 1 and Sys 2. Sys 1 and Sys 2 measurements were made on different test benches containing essentially the same instrumentation. This paper covers small signal analysis, power budgeting and power compression characteristics; amplitude and phase noise are not discussed. The component and subsystem measurement and simulation techniques should be of interest to anyone involved in development of RF/microwave front-end systems.

Component characterization

Our analysis of the subsystem shown in Figure 1 begins with a characterization of individual components. Shown in this section are the measurements for the hardware setup (Sys 1). Included are characterization results for the two amplifiers, the mixer and the two filters. The pads were also measured and found to be very close to the specified attenuation values.

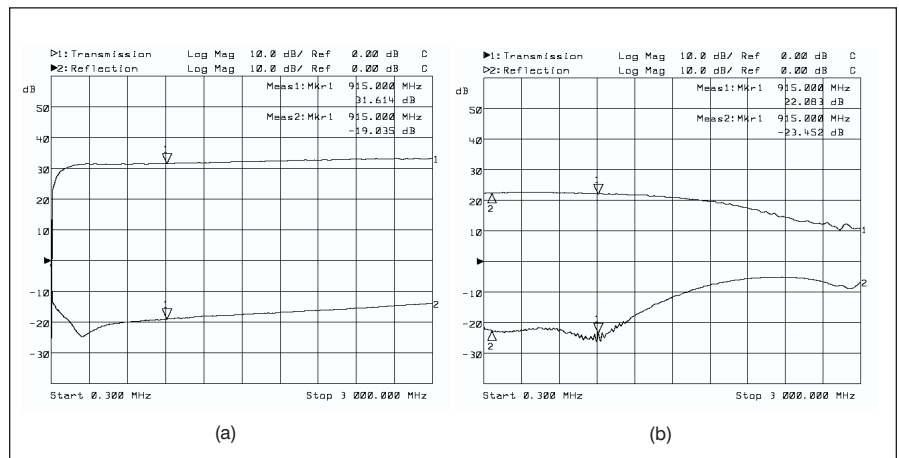
Amplifier characterization — The HP8714 VNA was used to measure the small signal characteristics of the two amplifiers in the subsystem [2,3]. One issue involved with amplifier characterization is that the input signal must be low enough to ensure linear operation of the DUT. The standard configuration for the HP8714 VNA does not include an internal attenuator, limiting the power range from -10 dBm to $+10$ dBm. Depending on the VNA options, external attenuation may be needed to achieve the proper DUT input level. The output signal level may also require external attenuation to keep it within the linear range of the VNA’s receiver.

Figure 3 shows the measured small signal responses for the two amplifiers. Reflection calibration for this, as well as the filter measurements shown later, was achieved using a 3.5 mm calibra-



▲ Figure 2. The basic test bench used for characterization of the 915 MHz receiver and its components.

tion kit’s short, open and load standards. Transmission calibration is achieved with a simple response calibration, using a through connection [3]. The measurements show that the Miteq amplifier (Figure 3a), although rated from 2 to 8 GHz, shows flat gain performance (31-32 dB) down to 150 MHz. In our receiver subsystem it provides a gain of about 31.6 dB at 915 MHz. The input return loss is better than 12 dB from 150 MHz to 3 GHz. The Mini-Circuits amplifier (Figure 3b) is rated to 1 GHz and has a measured gain of about 22 dB from 0.3 MHz to 1 GHz. The return loss is better than 15 dB across this frequency range. Regarding the receiver frequencies, both of these amplifiers can be considered broadband gain blocks, as they impose no frequency limits on the receiver. Moreover, the Mini-Circuits amplifier could be used in both the RF and IF amplifier positions, although subsystem performance would change.

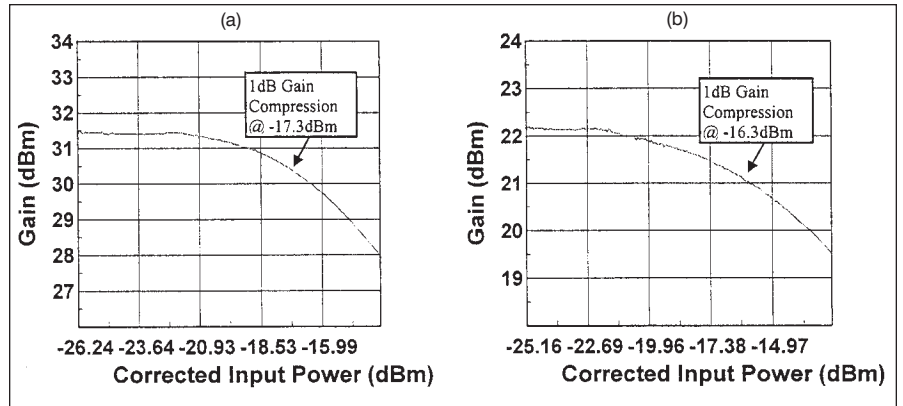


▲ Figure 3. Broadband (0-3000 MHz) measured transmission and reflection responses for the MITEQ (a) and Mini-Circuits (b) amplifiers. The markers are at 70 MHz and 915 MHz. The input signal level was about -30 dBm.

The 1 dB gain compression level (P_{1dB}) of the two amplifiers will play a role in determining the saturation characteristics of the receiver. Figure 4 shows the VNA measured results used to determine P_{1dB} for the RF and IF amplifiers. In each of the two diagrams, the gain is plotted as a function of corrected input power. The input power was corrected by directly measuring it, using the VNA's power measurement mode [3], with the input cable directly connected to the VNA test port.

For the RF amplifier (Figure 4a), the frequency was 915 MHz during the swept power measurement, while for the IF amplifier (Figure 4b) the frequency was 70 MHz. The results show an input P_{1dB} level of -17.3 dBm, or approximately $+13.1$ dBm output P_{1dB} , for the Miteq amplifier at 915 MHz. Similar measurement at 70 MHz on the Mini-Circuits amplifier produced a P_{1dB} referenced to the input of -16.3 dBm, which corresponds to an output P_{1dB} of 4.8 dBm.

Mixer characterization — There are many parameters of interest for a mixer, but in this article, we will restrict our attention to mixer conversion loss. Conversion loss is defined as the difference in dB between the power presented to the mixer RF port (at the RF frequency) and the power exiting the IF port (at the IF frequency). Conversion loss measurements were made in two different ways for the present application. In the first method, the broadband detection mode of the HP8714 VNA [2,3,4] was used. The RF signal was swept from 785 to 1485 MHz, with the LO frequency held at 985 MHz. This corresponds to IF frequencies ranging from 0 to 500 MHz. Accordingly, a 500 MHz lowpass filter was used in the IF cable during mixer measurement so that the VNA's broadband detector only responded to the desired IF signal. In the second method, the spectrum analyzer was used to make conversion loss measure-

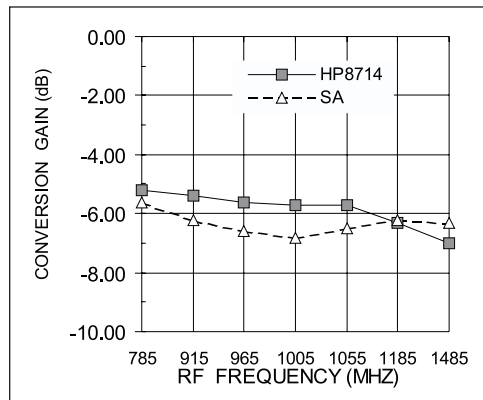


▲ Figure 4. Measurement of input 1 dB gain compression power for the 915 MHz RF amplifier (a) and 70 MHz IF amplifier (b).

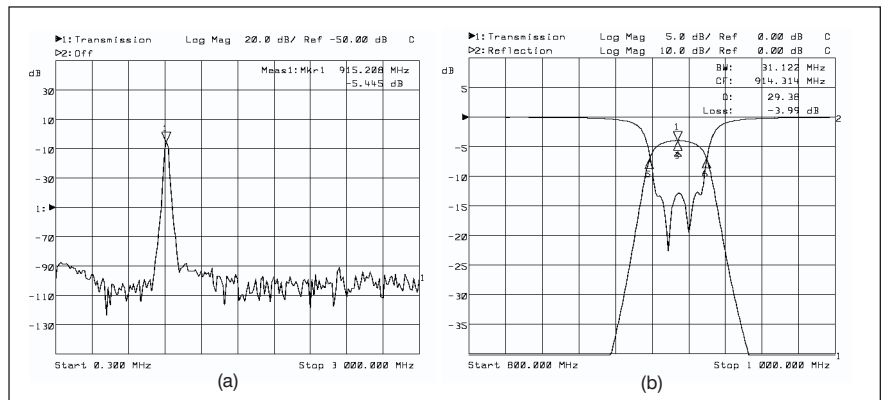
ments at a subset of the same frequencies.

With both methods, corrections have been applied to account for frequency dependent cable and filter losses [4]. The results from these two sets of measurements are shown in Figure 5. Note that conversion gain is plotted; this is the negative of conversion loss. The residual discrepancies in these measurements are due to inaccuracies and nonlinearities in the amplitude measurements made by SA and the VNA in broadband detector mode. Neither of these instruments are, by design, highly accurate power meters. As it is unclear which approach is more accurate, the average of the SA and VNA measurements of 5.8 dB, at 915 MHz, was used in the simulations.

The 1 dB compression level of the mixer was also measured. Using methods similar to that described above to characterize P_{1dB} for the amplifiers, the broadband detector mode of the VNA was used in conjunction with a power sweep to measure P_{1dB} for the mixer. In this case, the P_{1dB} corresponds to the power level at which the conversion loss increases by 1 dB over its small-signal value. Using an RF frequency of 915 MHz and an LO frequency of 985 MHz (at $+4$ dBm), a swept



▲ Figure 5. Mixer conversion loss measured with a VNA and SA. The LO is 985 MHz at $+4$ dBm; RF is -20 dBm.



▲ Figure 6. Measured response of the 915 MHz pre-select filter. The broadband response (a) shows out-of-band performance. Narrowband passband and return loss measurements are in (b).

915 MHz RECEIVER

power measurement yielded an input P_{1dB} of -1.7 dBm, corresponding to an output P_{1dB} IF power of -8.5 dBm.

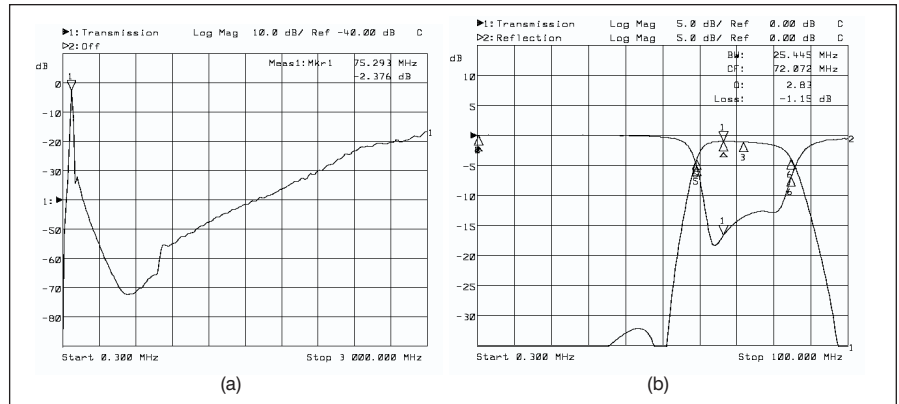
Filter characterization — VNA measurement of passive components, such as filters, is much more straightforward than the previously described amplifier and mixer measurements. One consideration for filter measurement is that both broadband and narrowband characteristics are usually of interest. Also, measurement averaging and isolation calibration may be necessary for accurate measurements of high out-of-band attenuation levels. Figure 6 shows the measured small-signal response for the 915 MHz filter, custom made by Piezo Technologies Inc. (PTI). The results show a 4 dB insertion loss, a 31 MHz bandwidth and out-of-band rejection levels of 90 dB. As a rule, in-band insertion loss is more accurately taken from a narrowband measurement, as the frequency resolution is improved.

The measured response of the 70 MHz IF filter is shown in Figure 7. The broadband response (a) shows that this filter's out-of-band rejection degrades to 16 dB at high RF frequencies. This problem can be overcome by cascading the filter with a lowpass filter to improve the signal purity of the IF output. The narrowband response in (b) shows an insertion loss of about 1 dB and a bandwidth of 25.5 MHz.

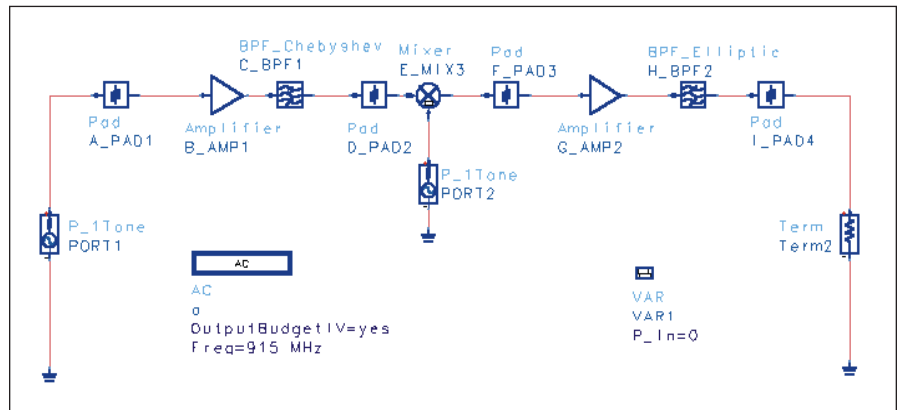
Simulation of the 915 MHz receiver

The capability to accurately simulate RF/microwave and signal processing components in a common CAD/CAE environment is a powerful tool for communication system design. In order to examine intermodulation distortion or adjacent channel power, for example, a simulation based on ideal filter performance may prove inadequate. A much more accurate prediction can be obtained by using actual filter characteristics, including the effects of non-ideal skirts and any parasitic passbands which may exist. The Advanced Design System (ADS) from Hewlett Packard provides this RF analog/digital cosimulation capability, enabling, for example, time-saving trade-off studies for the performance requirements on each side of a communications system. This portion of our article illustrates the use of the ADS software to simulate the performance of the 915 MHz receiver subsystem shown in Figure 1.

Our first simulation is a power budget analysis, useful for examining absolute power levels at specific points



▲ **Figure 7. Broadband (a) and narrowband (b) responses for the Mini-Circuits 70 MHz IF bandpass filter. The broadband response shows that out-of-band rejection degrades at high frequencies.**



▲ **Figure 8. Schematic used for the power budget analysis.**

in the receiver chain. The linear and non-linear swept frequency responses of the subsystem are simulated using the small- and large-signal sweep benches, respectively. Non-linear effects are also studied using the harmonic balance bench, in which a multitone excitation is demonstrated, along with the use of a mixer intermodulation table.

One of the topics addressed here is the use of the previously described component-level measured data in place of, or as a supplement to, the generic models available in the ADS libraries. Of particular importance at the system level is the non-ideal out-of-band performance of filters, which can best be represented by using measured s -parameters. It is equally important to accurately describe the non-linearities in the amplification and frequency-translation stages. This has been accomplished using measured or vendor-supplied specifications for the gain compression points of the amplifiers, and the intermodulation table for the mixer.

In addition to the components already described, the subsystem also includes attenuators at various points in the system. The 30 dB pad at the input in Figure 1 is

915 MHz RECEIVER

used to set a proper drive level for the receiver, based on the capability of the microwave sources available in the laboratory. The attenuators on either side of the mixer serve a similar purpose. The output (0.7 dB) pad is used to represent cable and connector losses that are present in the experimental setup.

Simulation results

Power budget — A small signal power budget analysis is useful for assessing the power flow through the system. The schematic representation of the system used in this simulation is shown in Figure 8. The ADS schematic includes all necessary information for running the

simulation. Table 1 shows the simulation results for a single 915 MHz tone. The first pad in the simulation is used to set the input power to the system during measurement but is not part of the receiver itself. Hence the input power to the system is -30.5 dBm. The output power is that delivered to Term2, -3.47 dBm. Measurements made on the sample receiver are included for comparison in Table 2. Convenient calculation of the internal power levels is important for maintaining linear operation of the active components of the system, namely the RF preamplifier, the mixer and the IF amplifier.

Small signal sweep — An efficient way to simulate the frequency-dependent, small-signal behavior of the system is with the small-signal sweep. The schematic used in this case is shown in Figure 9. Simulated results are shown in Figure 10, mea-

Component	Power at input
A_PAD1	0.00
B_AMP1	-30.5
C_BPF1	1.11
D_PAD2	-2.92
E_MIX3	-2.92
F_PAD3	-18.72
G_AMP2	-24.68
H_BPF2	-2.40
I_PAD4	-3.40
PORT1	0.00
PORT2	10.00
Term2	-3.47

▲ **Table 1. Results of the power budget simulation.**

Component	Simulated	Measured
Amplifier Input	-30.5	-30.5
Mixer Input	-12.92	-13
IF Filter Input	-2.4	-3.1
System Output	-3.47	-4.1

▲ **Table 2. Comparison between simulated and measured power levels.**

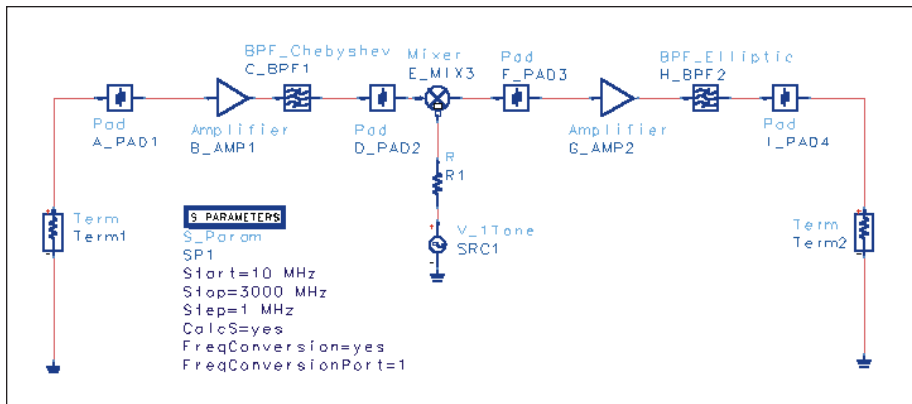
915 MHz RECEIVER

sured results in Figure 11, both including the 915 MHz pre-select filter. The simulation indicates a pass-band centered on the desired 915 MHz, with a much lower amplitude response when the RF is at the image frequency of 1055 MHz. The measurement for this case is limited in dynamic range by the broadband detector used in the network analyzer (the noise floor of the measurement is on the order of only 50 dBc) [1].

As shown in Figure 12, the measured response is significantly different when the 915 MHz pre-select filter is removed. Without this filter, strong responses are seen at the image frequency of 1055 MHz as well as at 2885 MHz, corresponding to $3f_{LO} - f_{IF}$. Note that the VCO output is unfiltered and has reasonably strong (~ 25 dBc) harmonic content at $2f_{LO}$ and $3f_{LO}$. As a result, without the RF pre-select filter, responses might be expected at $f_{LO} \pm f_{IF}$, $2f_{LO} \pm f_{IF}$, and $3f_{LO} \pm f_{IF}$. The corresponding frequencies are 915, 1055, 1900, 2040, 2885, and 3025 MHz. The mixer's double-balanced design suppresses the second harmonic response.

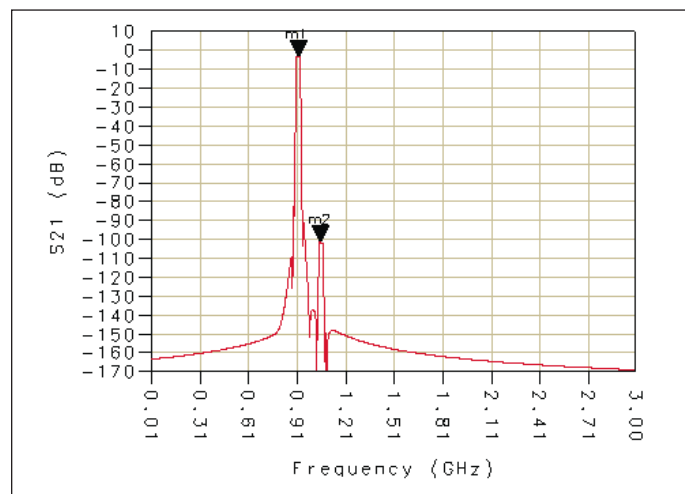
The simulated response without the RF filter, not shown here, predicts only the peaks at the 915 MHz frequency of interest and the image frequency of 1055 MHz. This is because of two simplifications in the simulation setup: The use of a simple mixer model, which does not account for intermodulation products; and the fact that the significant harmonic content of the LO signal is not modeled.

Large-signal sweep — A large signal sweep simulation can reveal the saturation or compression characteristics of the receiver. The ADS schematic used is shown in Figure 13, and the simulated results for a power sweep are shown along with measurements in Figure 14.

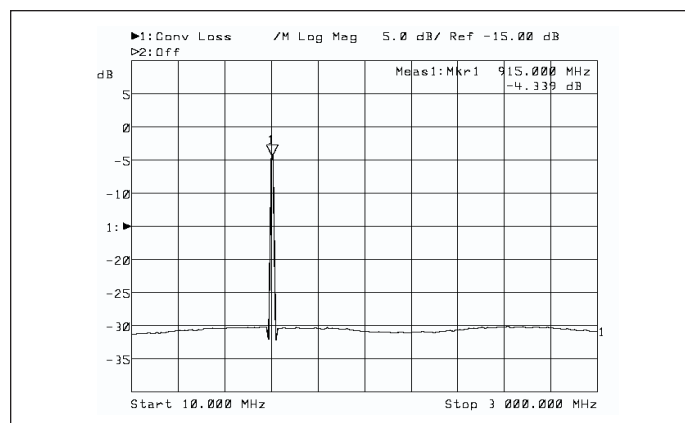


▲ Figure 9. Schematic used for the small signal sweep of the subsystem.

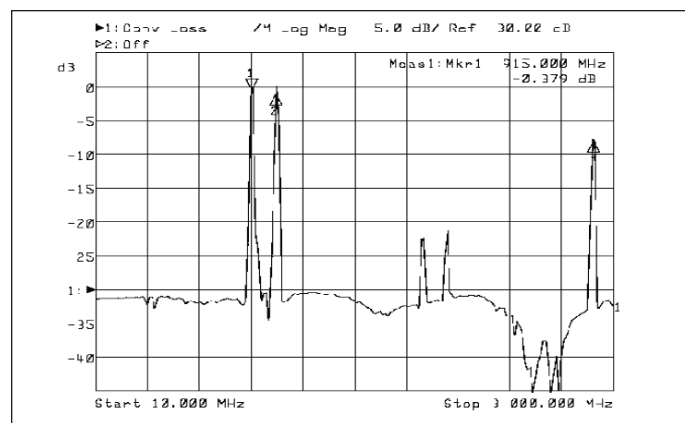
This sweep corresponds to a fixed RF frequency of 915 MHz, and shows the system to have a 1 dB compression of about 23 dBm, with agreement between measured and simulated sweep to within a tenth of a dB (certainly within the measurement accuracy).



▲ Figure 10. Simulated small-signal sweep results including the RF pre-select filter.



▲ Figure 11. Measured small-signal sweep results including the RF pre-select filter.



▲ Figure 12. Measured small-signal sweep results with the RF pre-select filter removed.

915 MHz RECEIVER

The input power plotted on the x-axis is the measured (or corrected) input power corresponding to the power sweep used. The nominal small-signal conversion gain is 27.0 dB with system input P_{1dB} power of -23.2 dBm. The corresponding output P_{1dB} power is: $-23.2 + 26.0 = +2.8$ dBm. The simulation relies on measured P_{1dB} values for the active components (amplifiers and mixer).

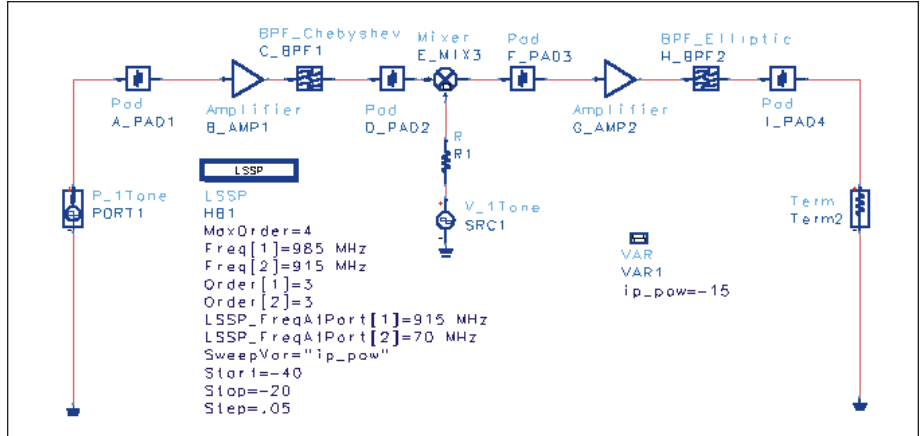
Harmonic balance simulation — A harmonic balance simulation can be used to investigate the nonlinear performance of a subsystem at user-specified input power levels. In the case of a frequency-translation application such as the 915 MHz receiver, it is particularly important to include a mixer IMT (intermodulation table) to account for mixer nonlinearities. The IMT is a file containing the amplitude of the intermodulation products for a given RF and LO frequency at specific power levels; for our design, the IMT data was provided by the manufacturer (Mini-Circuits).

When specifying the mixer parameters, it is also necessary to select the appropriate sideband to be used, upper or lower. Nonlinear effects in amplifiers can be treated by specifying the saturation parameters in the amplifier library model and by using database files that account for gain compression, power-dependent s -parameters, or s -parameters with gain compression.

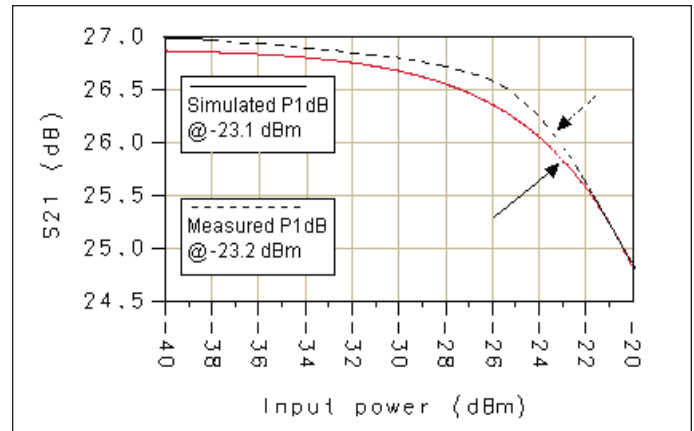
Another option that is available in harmonic balance simulation is the use of a multitone source at the RF and/or LO input. The different frequencies and their respective power levels are specified in the harmonic balance control item. (To improve the convergence of the solution, the component with the highest power level should be entered first in the list.) In the same menu, the user must specify the number of harmonics to be included. During the simulation, each input RF tone is treated separately, and the results available in the data display window are selected according to the individual RF frequency.

An example schematic using library models for the RF and IF filters, and the corresponding results from the harmonic balance simulation, are shown in Figures 15 and 16, respectively. In this case, the first and second harmonics are included in the multitone LO source. The most significant spurious products are $1 \times RF$, $1 \times LO$, $2 \times LO$ and $2 \times LO + RF$.

The simulation is made more real-

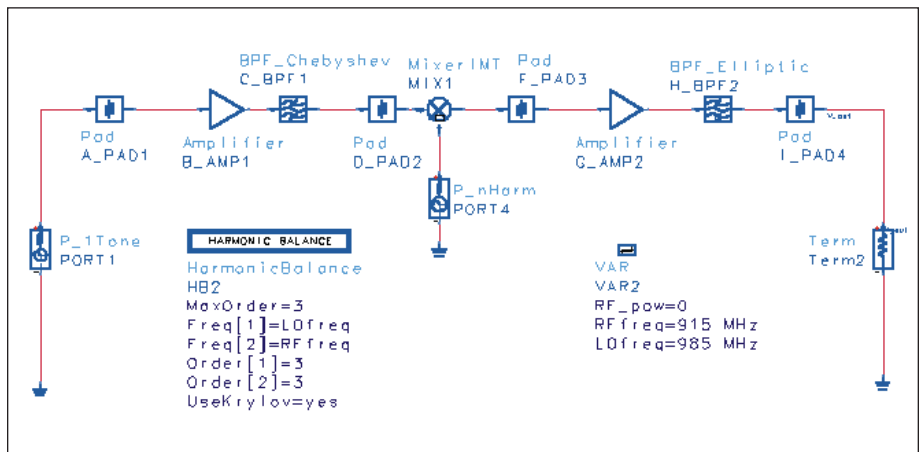


▲ Figure 13. Schematic used for the large-signal sweep of the subsystem.



▲ Figure 14. Simulated and measured large-signal sweep results. Note the close agreement.

istic by utilizing measured s -parameter data for the filters. This is particularly significant for representing accurate out-of-band performance, as can be seen by



▲ Figure 15. Schematic used for the harmonic balance simulation of the receiver, including a multitone local oscillator source. This simulation used library models for the RF and IF filters.

comparing measured and modeled filter responses, illustrated in Figures 17 and 18. The IF filter has the greatest effect in this simulation, since it sets the level of the harmonic output from the mixer. The degradation in the out-of-band rejection at the high end of the band due to the actual filter response is significant (Figure 18). A comparison between the two sets of simulated

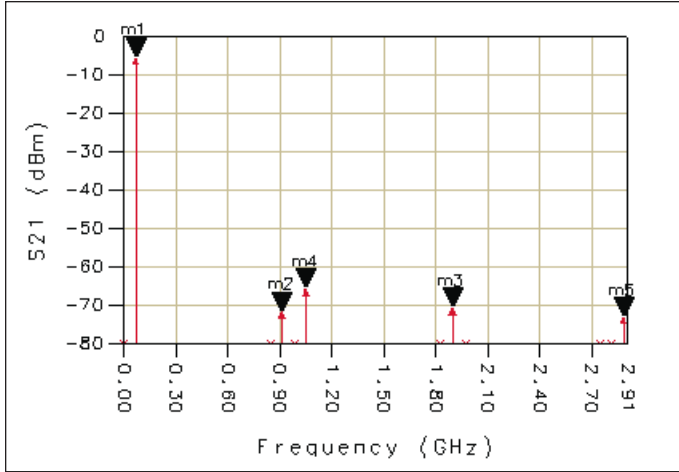
results (with library filter models and using measured filter data) is provided in Table 3. As would be predicted based on the filter differences, the harmonic levels are all higher when the measured data is used. This table also contains measurement data for the receiver subsystem. Some of the differences between this data and the predicted results may be due to the amplifier

gain specifications, which are assumed to be frequency-independent in the simulations.

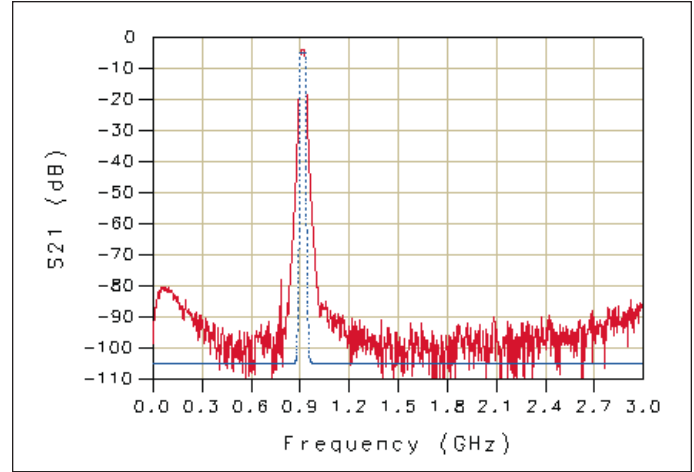
Receiver performance with signals received using an antenna

Performance with signals received using an antenna is the “bottom line” for a wireless receiver. As implied in Figure 2, a test was performed with a lab-generated transmit CW signal at 915 MHz. This was set up using an HP8648C signal generator connected to a log-periodic antenna. At a distance of approximately 18 feet, a monopole antenna was connected to the input of the receiver subsystem to pick up this signal along with whatever other signals were present in the local electromagnetic environment. An example of the input spectrum received by the antenna in the vicinity of 915 MHz is shown in Figure 19a. This was measured by connecting the receive antenna directly to the SA. Notice that, in addition to the lab-generated signal, strong peaks are seen in the range of 865 to 890 MHz, corresponding to local cellular telephone traffic, as well as even stronger peaks from 930 to 935 MHz from local paging signals.

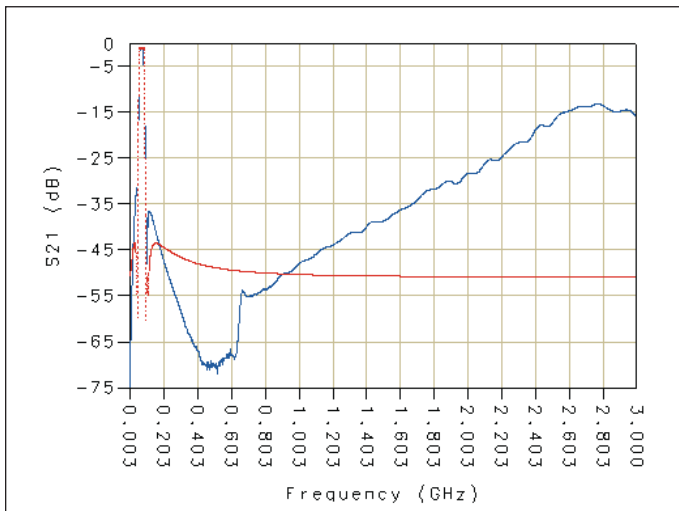
Connecting the antenna to the receiver input, and the receiver output to the SA, yields an IF spectrum similar to that shown in Figure 19b. With the exception of the band close to (e.g. ± 10 MHz) the lab-generated signal, the spectrum is dynamic; both plots shown in Figure 19 are snapshots of time varying spectral pictures. A strong peak is seen at the desired IF frequency of 70 MHz. There are also peaks in the neighborhood of 55 MHz and 93 MHz. These correspond to the paging and cell phone traffic, respectively. These signals are still observed in the IF spectrum since neither the RF nor the IF filter bandwidths are sufficiently narrow to reject these potentially interfering signals. A narrower band IF filter is being fabricated which will result in a cleaner IF spectrum.



▲ **Figure 16.** Simulation results for the harmonic balance analysis. The markers correspond to the following output products: $m1 = \text{IF}$, $m2 = \text{RF}$, $m3 = 2 \times \text{LO}$, $m4 = \text{LO}$, $m5 = 2 \times \text{LO} + \text{RF}$.



▲ **Figure 17.** Comparison between s_{21} for the library model of the RF filter and the measured frequency response of the filter used in the receiver.



▲ **Figure 18.** Comparison between s_{21} for the library model of the IF filter and the measured frequency response of the filter used in the receiver.

Frequency (MHz)	Simulated results: Library filter model (dBm)	Simulated results: Measured filters (dBm)	Measured data (dBm)
70	-4.05	-4.58	-4.6
915	-74.87	-64.73	-80.1
985	-86.65	-73.95	-75
1055	-103.5	-89.47	-85
1830	-102.07	-66.2	-72.6
1900	-69.19	-33.22	-49
1970	-122.85	-99.89	-60
2745	-102.81	-55.71	-90
2815	-118.98	-54.74	-77

▲ **Table 3.** Comparison of harmonic balance simulations using library models for the filters and using measured filter data, along with measured data for the subsystem.

Summary and Conclusions

A versatile test bench has been shown to be a useful tool for measurement characterization at the component and subsystem levels. When combined with simulation using modern CAE/CAD tools like HP's ADS, both linear and nonlinear characteristics can be examined and comparisons made with measured data.

In the area of the measurement system, the broadband detection mode and absolute power measurement features of the HP8714 VNA are valuable supplements to the conventional VNA tuned receiver mode. Accuracy limitations of the test bench exist in the areas of mixer and subsystem conversion loss or conversion gain measurements. While an uncertainty analysis is outside the

scope, experience suggest that these measurements probably cannot be specified any better than within ± 0.5 dB of the true values using the equipment and techniques applied. The addition of a calibrated power meter to the bench would allow more accurate conversion loss and absolute power measurements to be made at spot frequencies.

System modeling, as implemented, was found to be very useful for predicting the in-band characteristics of a frequency converting subsystem. Additional modeling complexity can also be added. For example, frequency-dependent s -parameters were not used for the RF and IF amplifiers, and a thorough noise analysis was not performed. However, there are clear advantages to the use

915 MHz RECEIVER

of simple built-in functional component models. The presented model was shown to be easily calibrated with measured data and demonstrated to produce useful simulations of swept response characteristics, power at various points in the system, and system 1 dB compression characteristics.

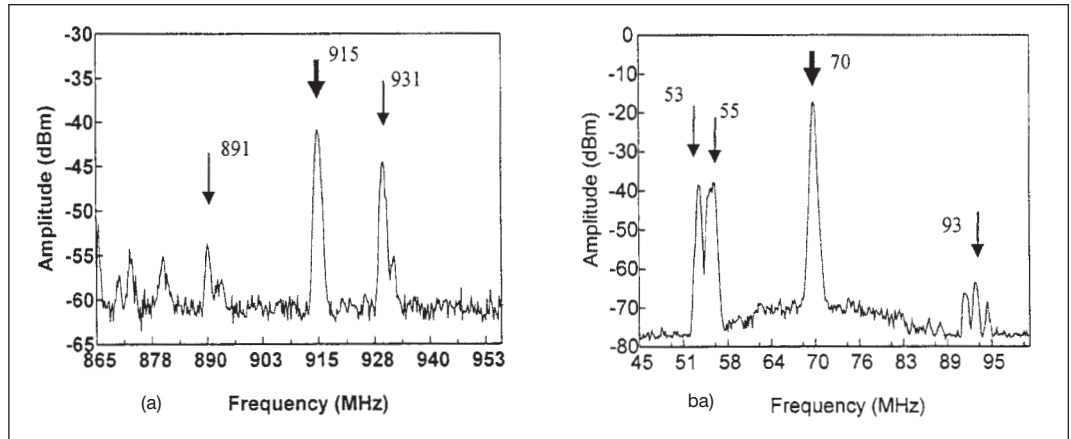
This study provides a basic foundation that can be built upon; for example, adding accurate treatment of noise figure would allow receiver sensitivity and dynamic range to be quantified.

Also, IF processing and demodulation circuitry can be added to the receiver hardware and/or associated simulation model. A similar approach can be followed to assemble a transmitter subsystem and model which could be used in concert with the receiver for complete wireless communication system measurement/simulation analyses.

The case study presented has excellent educational merits, providing an opportunity for system designers to gain experience with system hardware, software and instrumentation that could lead to more efficient measurement and simulation strategies for future designs. This study may also be used for short course and in-house training, in addition to its existing use in university instruction, where it already has proven to be extremely useful for training new RF engineers in the fundamentals of wireless and RF systems. ■

References

- 1.* P. G. Flikkema, L. P. Dunleavy, H. C. Gordon, R. E. Henning, T. M. Weller, "Wireless Circuit and System Design: A New Undergraduate Laboratory," *Proceedings of Frontiers in Education 1997*, November 5-8, 1997, Pittsburgh, PA.
- 2.* L. Dunleavy, "A Versatile Yet Economical Test Bench for Characterization of Wireless RF/Microwave Circuits and Systems," *Wireless and Microwave Technology 1997*, October 6-10, 1997, Chantilly, VA.
3. *HP8712B and HP8714B RF Network Analyzers*



▲ **Figure 19. RF input (a) and IF output (b) spectrum analyzer displays of the frequency and amplitude of the received spectrum, using an antenna to receive a 915 MHz test signal along with ambient signals. For (a), the receiving antenna is connected directly to the SA, while (b) was measured with the antenna connected to the subsystem input and the IF output connected to the SA.**

Users Guide, Hewlett Packard P/N 08712-90003.

4.* L. Dunleavy, T. Weller, E. Grimes and J. Culver, "Mixer Measurements Using Network and Spectrum Analysis," *48th ARFTG Conference*, December 5-6, 1996 Clearwater FL.

*These references are currently available from the WAMI web site: <http://www.eng.usf.edu/WAMI>

Acknowledgments

The equipment utilized in preparing this tutorial was made possible by combined grants from the National Science Foundation (Grant #DUE-9650529) and Hewlett Packard Company with matching funds from the University of South Florida. General support and assistance in the area of parts and supplies from the following companies is greatly appreciated: Mini-Circuits, Cushcraft, Miteq, and Piezo Technology Inc. We wish to acknowledge Rudy Henning and Horace Gordon of the University of South Florida who co-developed the WAMI lab with the first three authors.

Author information

The authors may be contacted at the Wireless and Microwave Instructional Laboratory, Department of Electrical Engineering, University of South Florida, 4202 E. Fowler Ave., ENB118, Tampa, FL 33620; Tel: (813) 974-2574; Fax: (813) 974-5250; Internet: <http://www.eng.usf.edu/WAMI>. E-mail may be sent to Lawrence Dunleavy at dunleavy@eng.usf.edu